

Intermediate- to high-energy positrons scattered by alkali-metal atoms

David D. Reid

Department of Physics and Astronomy, Eastern Michigan University, Ypsilanti, Michigan 48197

J. M. Wadehra

Department of Physics and Astronomy, Wayne State University, Detroit, Michigan 48202

(Received 31 December 1996; revised manuscript received 28 May 1997)

We present calculations of the differential, integrated elastic, and total cross sections for positrons scattered from alkali-metal atoms. The energy of the positrons ranges from 10 eV to 1000 eV. In the calculations we use parameter-free model potentials for the correlation-polarization and absorption interactions. The absorption potential used for positron scattering is based on a quasifree model that we recently proposed and tested for the noble-gas targets. For positron-alkali-metal scattering the model potentials have produced reliable scattering cross sections over the extended range of impact energies when compared against the available experimental data. [S1050-2947(98)00104-8]

PACS number(s): 03.80.+r

I. INTRODUCTION

In recent years positron-atom scattering has become a very interesting topic in both experimental and theoretical atomic collision studies. As an alternative to electron-atom scattering, both the similarities and the differences between electrons and positrons mean that positron scattering provides a useful, and sometimes more sensitive, test of the techniques used to study the electron-scattering processes.

This fact is particularly true from the standpoint of developing model interaction potentials for projectile-atom scattering. The similarities between electrons and positrons (mass, magnitude of charge, and spin) suggest that a consistent approach to devising model potentials should incorporate these quantities using similar logic for both projectiles. The differences between electrons and positrons, the sign of the charge, the possibility of positronium formation, and the fact that positron projectiles are distinguishable from the electrons of the target atom while electron projectiles are not offer important tests of how a model potential scheme handles issues such as projectile charge, inelastic thresholds, and correlations among projectile and target electrons. Therefore, model potentials that can reliably produce accurate scattering data for both electron- and positron-atom scattering signify an important step in our ability to perform these calculations quickly.

In the present paper, we use the model potential approach to calculate the differential, integrated elastic, and total cross sections for positron scattering from the alkali-metal atoms lithium, sodium, potassium, rubidium, and cesium at intermediate to high impact energies. The parameter-free model potentials that we employ in the present calculations are those that we have previously used, with good results, for positron scattering from the noble gases [1,2]. We have devised a model [1] for correlation and polarization effects to account for the distortion of the target atom under the influence of the electric field of the projectile. We have also introduced [2], for positron impact, a quasifree model potential for absorption effects to account for the inelastic scattering processes. The promising results that we have seen for

positron-noble-gas scattering have encouraged this present attempt to apply our models to a different atomic target group.

The set of alkali-metal atoms is an interesting alternative group to the noble gases for several reasons. As with the noble gases, the alkali-metal atoms have a simple, spherically symmetric ground-state structure that allows the use of central model potentials without appeal to angular averaging. Additionally, in recent years a body of experimental data has been building up for positron-alkali-metal scattering. Specifically, measurements of the total cross sections, which began in the 1980s [3], as well as measurements of positronium formation cross sections [4] continue until the present day. The primary reason, however, that we chose to follow our study of the noble gases by the alkali-metal atoms is because of their vastly different qualities. While the noble gases are tightly bound, closed-shell atoms with high inelastic thresholds, the alkali-metal atoms, all having unpaired electrons in the s subshell, are highly polarizable with positronium formation channels that are always open. This situation makes positron scattering from the alkali-metal atoms considerably more sensitive to the details of the model potentials than positron scattering from the noble gases is.

On the theoretical side, a number of calculations of cross sections, elastic as well as total, for positron-alkali-metal-atom systems at intermediate energies have been carried out. For the scattering of intermediate energy positrons by atomic lithium, elastic and/or total cross sections have been calculated by Tayal *et al.* [5], Wadehra [6], Khare and Vijayshri [7], Gien [8], Ward *et al.* [9], Mathur and Purohit [10], Basu and Ghosh [11], Hewitt *et al.* [12], and McAlinden *et al.* [13]. For positrons scattered by atomic sodium, calculations of cross sections have been made by Wadehra [6], Sarkar and Ghosh [14], Ward *et al.* [9], Gien [15], McCarthy *et al.* [16], and Hewitt *et al.* [17]. For positron scattering by potassium, various cross sections have been calculated by Wadehra [6], Ward *et al.* [9], Gien [15], McCarthy *et al.* [16], Hewitt *et al.* [17], Madison *et al.* [18], and McAlinden *et al.* [19]. For rubidium and cesium targets the calculations of intermediate-energy positron scattering cross sections are

TABLE I. Values of α_d , R_{orb} , and E_{excit} for various target atoms.

Target	α_d (a.u.)	R_{orb} (a.u.)	E_{excit} (eV)
lithium	164	3.0	1.85
sodium	163	3.2	2.11
potassium	293	4.1	1.62
rubidium	319	4.3	1.56
cesium	358	4.8	1.39

quite limited. For rubidium, various cross sections have been calculated by Wadehra [6], McEachran *et al.* [20], Gien [21] and Kernoghan *et al.* [22], and for cesium the calculations of cross sections are by Wadehra [6] and Kernoghan *et al.* [22].

The high polarizabilities of the alkali-metal atoms (see Table I), as compared to the noble gases, suggests a more important role for the polarization part of the correlation-polarization interaction V_{CP} , while the comparatively large size of the alkali-metal atoms (as “seen” by the large orbital radii listed in Table I) suggests a greater sensitivity to the correlation part of V_{CP} , which is our method for handling near-target distortion. The fact that the lowest inelastic threshold for positron–alkali-metal-atom scattering, corresponding to positronium formation, is zero poses an interesting problem in the quasifree absorption potential. As discussed in Ref. [2], this model was derived via a modification of a method used in nuclear physics for nucleon-nucleon scattering [23]. The necessary modification, for application to atomic scattering, was to introduce an energy gap Δ between the ground state of the atom and the first inelastic threshold [24]. When this energy gap is zero the resulting cross sections are infinite. However, in the case of positron scattering from alkali-metal atoms, as well as from noble-gas atoms, by simply using the lowest nonzero inelastic threshold one can produce reasonably accurate results for total cross sections over a wide energy range. In the case of noble-gas targets the lowest nonzero threshold corresponds to the positronium formation threshold [2] whereas in the case of alkali-metal atoms the lowest nonzero threshold corresponds to the lowest target excitation.

II. THEORY

A. Interaction potentials

In the present calculations we model the positron-target system by a complex interaction potential $V(r)$ that consists of only three parts. These parts are the static potential $V_{\text{st}}(r)$, the correlation-polarization potential $V_{\text{CP}}(r)$, and the absorption potential $V_{\text{abs}}(r)$, such that

$$V(r) = V_{\text{st}}(r) + V_{\text{CP}}(r) + iV_{\text{abs}}(r). \quad (1)$$

The static potential is determined by the radial part of the electron charge density of the target atom $\rho(r)$, which is obtained using the Hartree-Fock wave functions of Clementi and Roetti [25] for lithium, sodium, potassium, and rubidium and of McLean and McLean [26] for cesium. The static potential, in atomic units, is given by

$$V_{\text{st}}(r) = \frac{Z}{r} - 4\pi \int \frac{\rho(r')}{r_{>}} r'^2 dr', \quad (2)$$

where Z is the atomic number of the target atom and $r_{>}$ is the greater of r and r' .

The correlation-polarization interaction [1] is given by

$$V_{\text{CP}} = -\frac{\alpha_d r^2}{2(r^3 + d^3)^2}, \quad (3)$$

where k is the wave number of the incident positron and α_d is the static dipole polarizability of the target atom, respectively. The value of d , which is nonadjustable, is determined by matching the form in Eq. (3) with the correlation energy [27] at the location of the electron charge density peak of the outermost occupied orbital of the target; this value of r is the orbital radius of the atom R_{orb} . In Table I the values of α_d and R_{orb} for various alkali-metal atoms are provided. The values for α_d were taken from Ref. [28], while R_{orb} was determined using $\rho(r)$.

Note that Eq. (3) includes the static dipole part of the long-range potential. The higher-order multipole terms, behaving asymptotically like $1/r^6$, are not included for two reasons. First, the $1/r^6$ term contains dynamic contributions whose coefficients are, in general, not easily available for various targets. Second, inclusion of even the static contribution of this term, which contains the static quadrupole polarizability, did not contribute appreciably to the various cross sections in our calculations.

The final form of the absorption potential for positron-atom scattering was given in our previous work [2]; below we provide a sketch of its derivation. The quasifree scattering model starts by noting that a negative imaginary part of the interaction potential V_{abs} represents, in atomic units, an absorption probability per unit time of $-2V_{\text{abs}}$ [29]. This result is compared with the corresponding result from classical kinetic theory for a projectile in a free-electron gas of density ρ . For this latter case, the absorption probability per unit time is given by $\rho \bar{\sigma}_b v$, where v is the local speed of the projectile and $\bar{\sigma}_b$ is the average cross section for the binary collisions between the projectile positron and the target electrons. Thus we can write

$$V_{\text{abs}} = -\frac{1}{2} \rho \bar{\sigma}_b v. \quad (4)$$

The central problem in this model is to derive an expression for the average binary collision cross section $\bar{\sigma}_b$, which is given by the six-dimensional integral [23]

$$\bar{\sigma}_b = \frac{1}{p} \int N(k_F, q) |\mathbf{p} - \mathbf{q}| d\mathbf{q} \int \frac{d\sigma_b}{d\Omega} \times \left(\frac{1}{p_0^2} \delta(p_0 - p_f) \Theta(q', k_F) \right) d\mathbf{g}, \quad (5)$$

where \mathbf{p} and \mathbf{q} are the laboratory frame momenta of the incident positron and of the target electron, respectively, before the collision; \mathbf{p}' and \mathbf{q}' are the laboratory frame momenta of the incident positron and of the target electron,

respectively, after the collision. The vectors \mathbf{p}_0 and \mathbf{p}_f are the initial and final momenta of the positron in the center-of-mass frame of the binary system. The function $N(k_F, q)$ is the density per target electron in momentum space; it is given by

$$N(k_F, q) = \begin{cases} \frac{3}{4\pi k_F^3}, & q \leq k_F \\ 0, & q > k_F, \end{cases} \quad (6)$$

where $k_F = (3\pi^2\rho)^{1/3}$ is the Fermi momentum of the target. The momentum transfer vector \mathbf{g} is given by $\mathbf{g} = \mathbf{p}' - \mathbf{p} = \mathbf{q} - \mathbf{q}'$. The binary collision occurs between the incident positron and a target electron; in analogy with the electron scattering case, the differential binary cross section is based on the Rutherford formula as

$$\frac{d\sigma_b}{d\Omega} = \frac{2}{g^4}. \quad (7)$$

The function $\Theta(q', k_F)$ in Eq. (5) is unity for allowed final states of the binary collision and zero for final states that are not allowed because of the Pauli exclusion principle. For positron-atom scattering this function is

$$\Theta(q', k_F) = H(q'^2 - k_F^2 - \omega), \quad (8)$$

where ω is given by $\omega = 2\Delta$, with Δ the energy gap between the target ground-state energy and the final energy of the originally bound target electron; $H(q'^2 - k_F^2 - \omega)$ is the Heaviside unit step function, which equals 1 when the argument is non-negative and zero otherwise.

The physical interpretation of $\Theta(q', k_F)$ is that for an elastic process to occur the final energy of the target electron $q'^2/2$ must exceed the Fermi energy $E_F = k_F^2/2$ by at least the energy gap Δ . Processes that would allow the electron to fall into a lower-energy state are forbidden due to *Pauli blocking*. The above definition of the Pauli blocking function Θ differs from that used for electron scattering [24] in that here, for positron scattering, Pauli blocking restrictions are applied to the target electrons only and no such restrictions are placed on the projectile.

It is interesting to examine the role of the energy gap Δ in the model for positron scattering as compared to its role in the quasifree model for electron scattering. For incident electrons Δ acts both as the energy needed to transfer a target electron from the highest occupied ground-state orbital to the first excited orbital and as the nonzero threshold for inelastic scattering. However, for incident positrons this situation is complicated since the formation of positronium introduces another bound system, the binding energy of which can reduce the inelastic threshold to an energy below the threshold for excitation E_{excit} . In fact, the quasifree absorption potential gives infinite cross sections as Δ approaches zero. In our calculations of positron scattering from noble gases [2] we used for Δ the nonzero positronium formation threshold E_{Ps} . In the case of positron scattering from alkali-metal atoms E_{Ps} is zero and in order to apply the quasifree model to positron scattering from alkali-metal atoms we set Δ equal to the lowest nonzero inelastic threshold, which is the excitation

thresholds E_{excit} , for these atoms. The values of E_{excit} for various alkali-metal atoms are also provided in Table I [30].

The total interaction potential in Eq. (1) is placed in the radial Schrödinger equation and integrated out to a distance of 120 a.u. from the nucleus via the Numerov technique. Several phase shifts are calculated exactly by comparing u_ℓ , the radial wave function of the target plus positron system, at two adjacent points r and $r_+ = r + h$:

$$\tan(\delta_\ell) = \frac{r_+ u_\ell(r) j_\ell(kr_+) - r u_\ell(r_+) j_\ell(kr)}{r u_\ell(r_+) n_\ell(kr) - r_+ u_\ell(r) n_\ell(kr_+)}, \quad (9)$$

where h is the step size (≥ 0.00075 a.u.) of the calculation and j_ℓ and n_ℓ are the spherical Bessel and Neumann functions evaluated using the algorithm of Gillman and Fiebig [31]. Typically, the highest order of the exact phase shifts ℓ_{max} is taken to be 50 for $E \leq 100$ eV and is taken to be 70 for $100 \text{ eV} < E \leq 1000$ eV, where E is the incident positron energy.

The scattering amplitude is obtained from the phase shifts by

$$f(\theta) = \frac{1}{2ik} \sum_{\ell=0}^{\ell_{\text{max}}} (2\ell+1) [\exp(2i\delta_\ell) - 1] P_\ell(\cos\theta) + f_4(\theta). \quad (10)$$

The function f_4 is the higher- ℓ contribution from the Born phase shifts for the dipole ($\sim 1/r^4$) part of the polarization potential. The closed form expression, in atomic units, for this function is [32]

$$f_4(\theta) = -\pi k \alpha_d \left(\frac{\sin(\theta/2)}{2} + \sum_{\ell=0}^{\ell_{\text{max}}} \frac{P_\ell(\cos\theta)}{(2\ell+3)(2\ell-1)} \right). \quad (11)$$

The differential and integrated elastic cross sections are obtained from the scattering amplitude in the usual manner

$$\frac{d\sigma}{d\Omega} = |f(\theta)|^2 \quad (12)$$

and

$$\sigma_{\text{elas}} = 2\pi \int |f(\theta)|^2 \sin(\theta) d\theta. \quad (13)$$

The total cross sections are calculated using the optical theorem

$$\sigma_{\text{tot}} = \frac{4\pi}{k} \text{Im}[f(0)]. \quad (14)$$

B. Binary collision cross section

As stated above, evaluation of the integral in Eq. (5) is the central problem of the quasifree scattering model. In the present evaluation of this integral for positron scattering we will use a notation, as well as a procedure, very similar to that for the electron-scattering case [24]. We note that the motion of the center of mass of the positron and the target electron implies that

$$\mathbf{p}_0 = \frac{\mathbf{p} - \mathbf{q}}{2}, \quad \mathbf{p}_f = \frac{\mathbf{p}' - \mathbf{q}'}{2}, \quad \mathbf{g} = \mathbf{p}_f - \mathbf{p}_0. \quad (15)$$

Using these relations along with the result $\delta(p_0 - p_f) = 2p_0 \delta(p_0^2 - p_f^2)$, Eq. (5) becomes

$$\bar{\sigma}_b = \frac{8N(k_F, q)}{p} \int \frac{d\mathbf{g}}{g^4} \int d\mathbf{q} H(q'^2 - k_F^2 - \omega) \times H(k_F - q) \delta(p_0^2 - p_f^2), \quad (16)$$

where we have added an additional step function $H(k_F - q)$ to account for the fact that $N(k_F, q)$ is zero if $q > k_F$.

The integral over \mathbf{q} can be evaluated in cylindrical coordinates with $d\mathbf{q} = q_R dq_R dq_\phi dq_z$, $q^2 = q_R^2 + q_z^2$, and the z axis antiparallel to \mathbf{g} . Having evaluated this integral, the binary cross section can be written as

$$\bar{\sigma}_b = \frac{8\pi N(k_F, q)}{p} \int \frac{d\mathbf{g}}{g^5} H(k_F^2 - (\mathbf{g} + \hat{\mathbf{g}} \cdot \mathbf{p})^2) \times H(-g^2 - 2\mathbf{g} \cdot \mathbf{p} - \omega) \{k_F^2 - (\mathbf{g} + \hat{\mathbf{g}} \cdot \mathbf{p})^2 + H(k_F^2 + \omega - (\hat{\mathbf{g}} \cdot \mathbf{p})^2) [(\hat{\mathbf{g}} \cdot \mathbf{p})^2 - k_F^2 - \omega]\}. \quad (17)$$

However, the integral over \mathbf{g} is most conveniently evaluated using spherical coordinates. The procedure is lengthy but straightforward [33]. Several cancellations produce a rather compact expression for the binary collision cross section for positrons. For the convenience of showing this result, we define

$$\delta = \frac{\omega}{2E_F}, \quad \varepsilon = \sqrt{\frac{E}{E_F}}, \quad (18)$$

and

$$f(x) = \frac{2}{\delta} x^3 + 6x + 3\varepsilon \ln \left(\frac{\varepsilon - x}{\varepsilon + x} \right). \quad (19)$$

Then the absorption potential is given by Eq. (4) with

$$\bar{\sigma}_b = \frac{\pi}{(\varepsilon E_F)^2} \times \begin{cases} f(0), & \varepsilon^2 - \delta \leq 0 \\ f(\sqrt{\varepsilon^2 - \delta}), & 0 < \varepsilon^2 - \delta \leq 1 \\ f(1), & 1 < \varepsilon^2 - \delta. \end{cases} \quad (20)$$

Here E_F is in units of hartree and $\bar{\sigma}_b$ is in units of a_0^2 .

III. RESULTS AND DISCUSSION

Figures 1–4 show the present results for the integrated elastic and total cross sections for scattering of positrons from lithium, sodium, potassium, rubidium, and cesium, respectively, compared with the available experimental data. On the experimental side, the total cross sections for the scattering of positrons, in the energy range 3–102 eV, from sodium, potassium, and rubidium have been measured recently [34–36]. The total experimental uncertainties in the positron scattering cross sections, shown by the error bars in Figs. 1–4, are estimated to be 21% [34–36]. Also, the first measurements of the positronium formation cross sections in

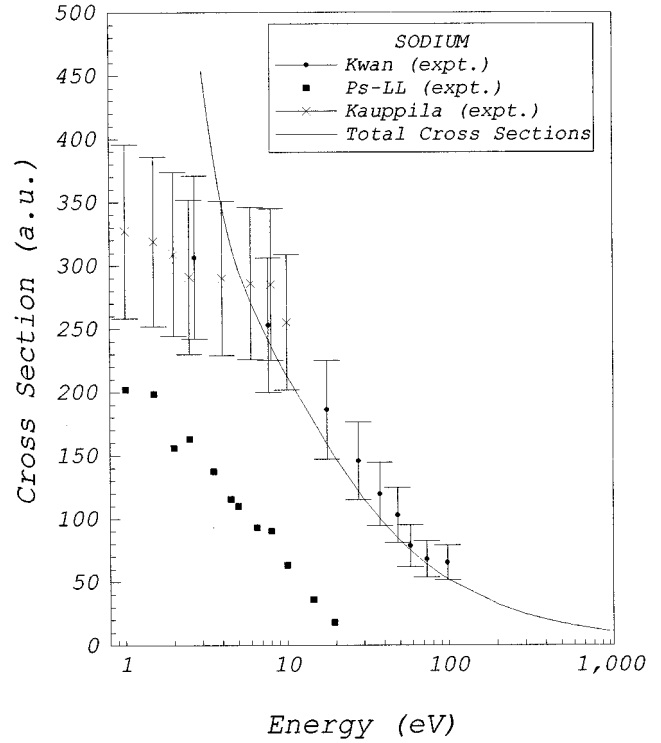


FIG. 1. Total cross sections for positron-sodium scattering. The experimental total cross sections are taken from Kwan *et al.* [34] and Kauppila *et al.* [36]. The Ps-LL data are the lower-limit estimates (more accurate) for the positronium formation cross sections [4].

the scattering of positrons by sodium (1–20 eV), potassium (1–100 eV), and rubidium (1–17 eV) have been reported recently [4,37].

The present results for various cross sections are shown for the positron energy range ~ 10 –1000 eV. This is the range in which the present results are expected to be most accurate because for the cases of sodium, potassium, and rubidium [4,37] the range $E \geq 20$ eV is beyond the energy region in which positronium formation is its most important, we also expect this to be the case for lithium and cesium. In our previous calculations for scattering of positrons from the noble gases we noticed that our calculations were least accurate in the energy region near and below the peak in the positronium formation cross sections. Well below 20 eV the present theoretical cross sections become quite large (see Table II) and considerably overestimate any measured values. This behavior is consistent with other previous theoretical calculations [9,38] in which positronium formation was not included. However, recent coupled-state calculations of positron scattering by potassium [19], taking the positronium channels into account, indeed show a pronounced peak in the total cross sections around 6 eV. This peak is largely attributed to the inclusion of positronium formation channels. Although we do not have experimental data for positron scattering from lithium and cesium, it seems reasonable to believe that the same general features are true for these target atoms as well. Numerical values of the integrated elastic and total cross sections for the scattering of 10–1000 eV posi-

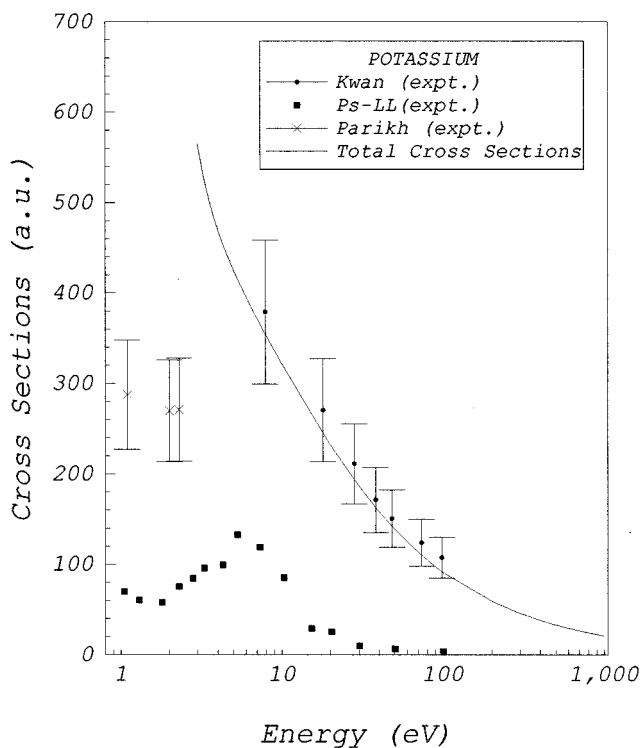


FIG. 2. Total cross sections for positron-potassium scattering. The experimental total cross sections are taken from Kwan *et al.* [34] and Parikh *et al.* [35]. The Ps-LL data are the lower-limit estimates (more accurate) for the positronium formation cross sections [4].

trons from the five alkali-metal atoms are provided in Table II.

As far as a comparison of our calculations with other work is concerned, we note that the present total cross sections for all five alkali-metal targets are in reasonable agreement with previous calculations as well as with the corresponding experimental data as shown in the figures. However, our integrated elastic cross sections differ from those in the other calculations. The majority of the previous positron-alkali-metal-atom elastic scattering cross section calculations are done for the positron energy less than 100 eV. In this energy range, our elastic cross sections are typically larger, almost by a factor of 2, than the other calculated elastic cross sections for Li [5,9,11,12], Na [9,17], K [9,17], Rb [20,22], and Cs [22]. To date, no experimental measurements of the integrated cross sections for elastic scattering of positrons by any alkali-metal atom have been carried out and therefore no direct comparison of our elastic cross sections with any experimental data is possible at the present time.

Figures 5 and 6 show our predicted values for the differential cross sections (DCSs) at 100 eV positron energy. We present these results for all five alkali-metal atom targets in the hope that future measurements will check the accuracy and the predictive power of the parameter-free model potentials. Our calculations show structure in the DCS curves, between 20° and 80° , which becomes more pronounced with increasing atomic number. For all the targets considered here the DCS curves flatten at scattering angles larger than 80° . While it is clear that this structure is due to interference effects, the precise physics of how and where the local

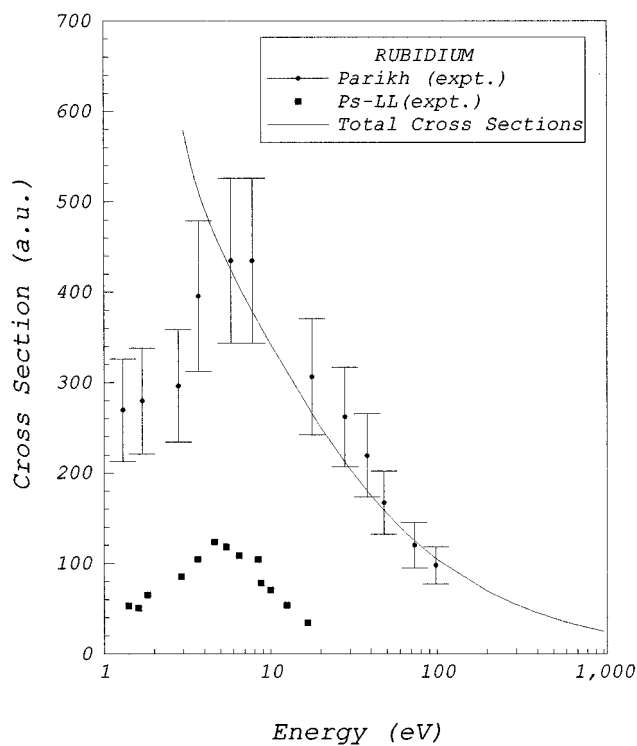


FIG. 3. Total cross sections for positron-rubidium scattering. The experimental total cross sections are taken from Parikh *et al.* [35]. The Ps-LL data are the lower-limit estimates (more accurate) for the positronium formation cross sections [36].

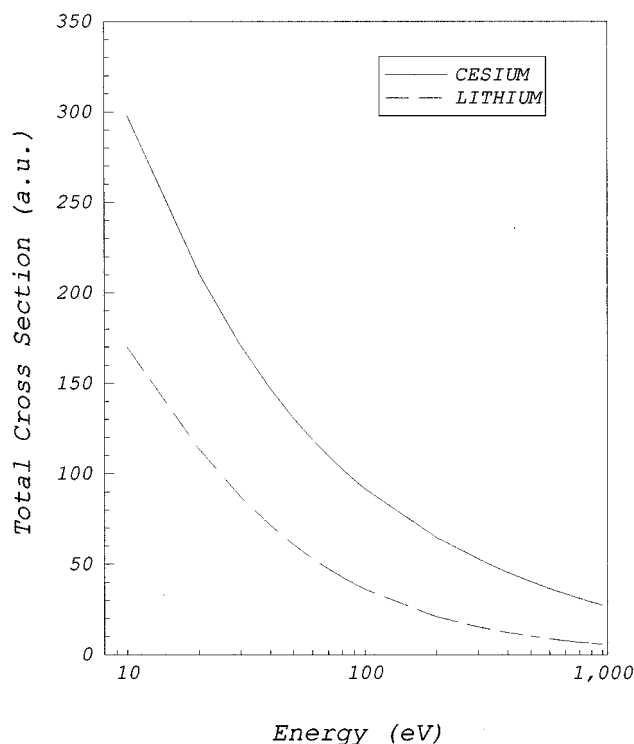


FIG. 4. Total cross sections for positron-lithium and positron-cesium scattering.

TABLE II. Present integrated elastic and total cross sections for positron-alkali-metal scattering in units of a_0^2 . The notation $a[b]$ means $a \times 10^b$.

E (eV)	Lithium		Sodium		Potassium		Rubidium		Cesium	
	Elastic	Total	Elastic	Total	Elastic	Total	Elastic	Total	Elastic	Total
10	7.55[1]	1.70[2]	1.09[2]	2.13[2]	1.69[2]	3.21[2]	1.76[2]	3.43[2]	1.20[2]	2.98[2]
20	4.68[1]	1.14[2]	7.47[1]	1.48[2]	1.24[2]	2.32[2]	1.31[2]	2.51[2]	8.17[1]	2.11[2]
30	3.40[1]	8.72[1]	5.81[1]	1.15[2]	1.00[2]	1.87[2]	1.08[2]	2.04[2]	6.47[1]	1.71[2]
40	2.69[1]	7.14[1]	4.80[1]	9.60[1]	8.52[1]	1.58[2]	9.28[1]	1.75[2]	5.50[1]	1.47[2]
50	2.23[1]	6.08[1]	4.12[1]	8.29[1]	7.46[1]	1.39[2]	8.20[1]	1.55[2]	4.85[1]	1.31[2]
60	1.91[1]	5.31[1]	3.62[1]	7.33[1]	6.66[1]	1.25[2]	7.40[1]	1.40[2]	4.38[1]	1.19[2]
70	1.68[1]	4.73[1]	3.24[1]	6.60[1]	6.04[1]	1.13[2]	6.76[1]	1.28[2]	4.03[1]	1.10[2]
80	1.49[1]	4.28[1]	2.94[1]	6.03[1]	5.55[1]	1.04[2]	6.24[1]	1.19[2]	3.75[1]	1.03[2]
90	1.35[1]	3.91[1]	2.70[1]	5.56[1]	5.14[1]	9.72[1]	5.81[1]	1.11[2]	3.52[1]	9.67[1]
100	1.23[1]	3.61[1]	2.50[1]	5.17[1]	4.79[1]	9.11[1]	5.45[1]	1.04[2]	3.32[1]	9.17[1]
200	6.77[0]	2.10[1]	1.50[1]	3.23[1]	2.99[1]	5.92[1]	3.48[1]	6.93[1]	2.29[1]	6.48[1]
300	4.78[0]	1.53[1]	1.10[1]	2.46[1]	2.24[1]	4.59[1]	2.64[1]	5.42[1]	1.84[1]	5.28[1]
400	3.74[0]	1.22[1]	8.91[0]	2.03[1]	1.81[1]	3.82[1]	2.15[1]	4.54[1]	1.57[1]	4.55[1]
500	3.09[0]	1.02[1]	7.54[0]	1.75[1]	1.53[1]	3.31[1]	1.83[1]	3.94[1]	1.39[1]	4.04[1]
600	2.64[0]	8.81[0]	6.57[0]	1.55[1]	1.33[1]	2.93[1]	1.59[1]	3.50[1]	1.26[1]	3.66[1]
700	2.31[0]	7.77[0]	5.84[0]	1.40[1]	1.18[1]	2.64[1]	1.42[1]	3.17[1]	1.56[1]	3.36[1]
800	2.06[0]	6.95[0]	5.28[0]	1.28[1]	1.07[1]	2.41[1]	1.28[1]	2.89[1]	1.08[1]	3.12[1]
900	1.87[0]	6.29[0]	4.82[0]	1.18[1]	9.74[0]	2.22[1]	1.18[1]	2.67[1]	1.02[1]	2.91[1]
1000	1.71[0]	5.75[0]	4.45[0]	1.10[1]	8.97[0]	2.06[1]	1.08[1]	2.48[1]	9.66[0]	2.74[1]

minima arise in differential cross sections at intermediate energies is not well understood to date. Recently, an attempt to explain such structure for *electron* scattering was put forth by Egelhoff [39] using a semiclassical approach. This semiclassical explanation, however, does not account for the structure seen in positron-atom differential cross sections.

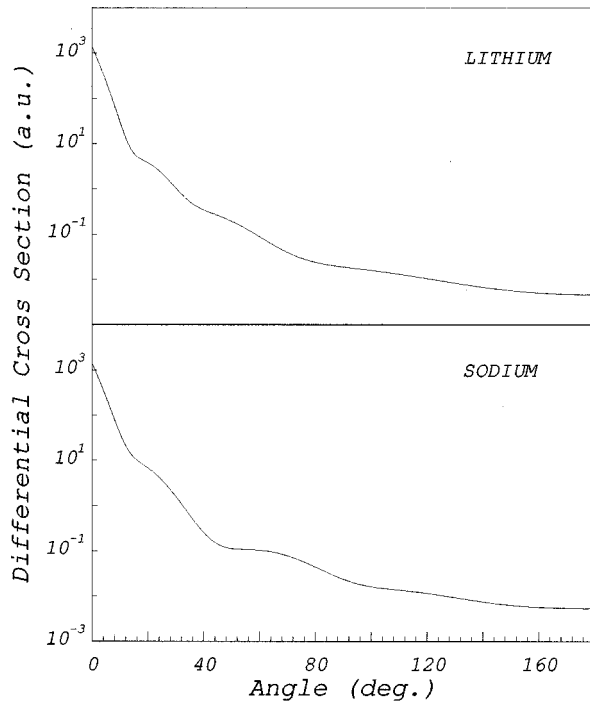


FIG. 5. Differential cross sections for elastic positron scattering from lithium and sodium at 100 eV impact energy.

We expect that there is a general explanation that accounts for the locations of the minima in both electron and positron scattering data; to date this general explanation has not been worked out.

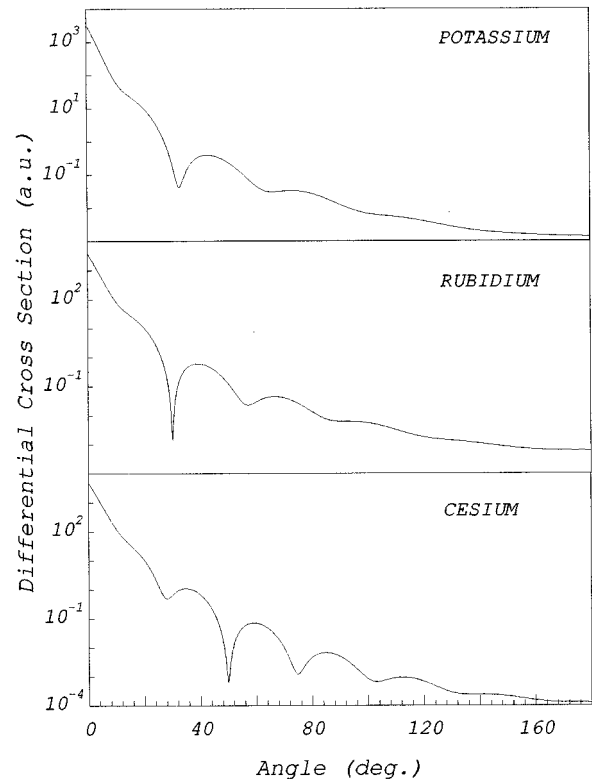


FIG. 6. Differential cross sections for elastic positron scattering from potassium, rubidium, and cesium at 100 eV impact energy.

One of the most interesting aspects of this study is that the use of the quasifree absorption potential remains a viable option for positron scattering from alkali-metal atoms despite the fact that the positronium formation channel for these systems is always open. Thus, for alkali-metal atoms the appropriate choice of Δ is $\Delta = E_{\text{excit}}$ that is the lowest nonzero inelastic threshold. For comparative purposes we note that for noble gas targets the choice $\Delta = E_{\text{excit}}$ leads to cross sections which are in good agreement with the available experimental data except near threshold energies. However, the choice $\Delta = E_{\text{ps}}$ for noble-gas targets leads to cross sections that are in better agreement with the corresponding experimental data as presented in Ref. [2]. This fact suggests that the lowest nonzero inelastic threshold energy is indeed the proper choice for Δ .

In this paper we have extended our investigations of the applicability of parameter-free model potentials for correlation-polarization effects and for absorption effects in positron-atom scattering. The present calculations test more stringently the features of these model potentials and suggest that these potentials can produce reliable total cross sections for positron-atom scattering at impact energies above the region where the process of positronium formation reaches its

peak. When taken together with our previous calculations for positron scattering from the noble gases [1,2], the present results suggest that our model potentials are useful for atomic targets with (a) small and large atomic numbers, (b) small and large orbital radii, (c) small and large polarizabilities, and (d) inelastic thresholds that extend all the way down to zero impact energy. Hence we believe that our present models, which are not fitted to experimental results by continuous adjustment of any parameters, serve as excellent starting points from which to pursue a globally applicable total interaction potential. In the interim, the total interaction potential as presently formulated is quite useful, as an applied physics tool, for fast computation of scattering data extending from the difficult intermediate-energy range (where both low- and high-energy approximations may fail) up to high impact energies.

ACKNOWLEDGMENTS

We gratefully acknowledge the support of National Science Foundation for this work. We also thank Professor W. E. Kauppila and Professor T. S. Stein for providing useful information.

-
- [1] D. D. Reid and J. M. Wadehra, *Phys. Rev. A* **50**, 4859 (1994).
 [2] D. D. Reid and J. M. Wadehra, *J. Phys. B* **29**, L127 (1996); **30**, 2318 (1997).
 [3] T. S. Stein, R. D. Gomez, Y.-F. Hsieh, W. E. Kauppila, C. K. Kwan, and Y. J. Wan, *Phys. Rev. Lett.* **55**, 488 (1985).
 [4] S. Zhou, S. P. Parikh, W. E. Kauppila, C. K. Kwan, D. Lin, A. Surdutovich, and T. S. Stein, *Phys. Rev. Lett.* **73**, 236 (1994).
 [5] S. S. Tayal, A. N. Tripathi, and M. K. Srivastava, *Phys. Rev. A* **24**, 1817 (1981).
 [6] J. M. Wadehra, *Can. J. Phys.* **60**, 601 (1982).
 [7] S. P. Khare and Vijayshri, *J. Phys. B* **16**, 3621 (1983).
 [8] T. T. Gien, *J. Phys. B* **22**, L463 (1989).
 [9] S. J. Ward, M. Horbatsch, R. P. McEachran, and A. D. Stauffer, *J. Phys. B* **22**, 1845 (1989).
 [10] K. C. Mathur and S. P. Purohit, *Phys. Rev. A* **42**, 2696 (1990).
 [11] M. Basu and A. S. Ghosh, *Phys. Rev. A* **43**, 4746 (1991).
 [12] R. N. Hewitt, C. J. Noble, and B. H. Bransden, *J. Phys. B* **25**, 2683 (1992).
 [13] M. T. McAlinden, A. A. Kernoghan, and H. R. J. Walters, *J. Phys. B* **30**, 1543 (1997).
 [14] K. P. Sarkar and A. S. Ghosh, *J. Phys. B* **22**, 105 (1989).
 [15] T. T. Gien, *J. Phys. B* **24**, 2871 (1991).
 [16] I. E. McCarthy, K. Ratnavelu, and Y. Zhou, *J. Phys. B* **26**, 2733 (1993).
 [17] R. N. Hewitt, C. J. Noble, and B. H. Bransden, *J. Phys. B* **26**, 3661 (1993).
 [18] D. H. Madison, M. Lehmann, R. P. McEachran, and K. Bartschat, *J. Phys. B* **28**, 105 (1995).
 [19] M. T. McAlinden, A. A. Kernoghan, and H. R. J. Walters, *J. Phys. B* **29**, 555 (1996).
 [20] R. P. McEachran, M. Horbatsch, and A. D. Stauffer, *J. Phys. B* **24**, 1107 (1991).
 [21] T. T. Gien, *J. Phys. B* **26**, 3653 (1993).
 [22] A. A. Kernoghan, M. T. McAlinden, and H. R. J. Walters, *J. Phys. B* **29**, 3971 (1996).
 [23] M. L. Goldberger, *Phys. Rev.* **74**, 1269 (1948).
 [24] G. Staszewska, D. W. Schwenke, D. Thirumalai, and D. G. Truhlar, *Phys. Rev. A* **28**, 2740 (1983).
 [25] E. Clementi and C. Roetti, *At. Data Nucl. Data Tables* **14**, 177 (1974).
 [26] A. D. McLean and R. S. McLean, *At. Data Nucl. Data Tables* **26**, 207 (1981).
 [27] A. Jain, *Phys. Rev. A* **41**, 2437 (1990).
 [28] E. W. McDaniel, *Atomic Collisions: Electron and Photon Projectiles* (Wiley, New York, 1989).
 [29] L. I. Schiff, *Quantum Mechanics* (McGraw-Hill, New York, 1968).
 [30] Charlotte E. Moore, *Atomic Energy Levels*, Nat. Bur. Stand. (U.S.) Circ. No. 467 (U.S. GPO, Washington, DC, 1949, Vols. I–III).
 [31] E. Gillman and H. R. Fiebig, *Comput. Phys.* **2**, 62 (1988).
 [32] J. M. Wadehra and S. N. Nahar, *Phys. Rev. A* **36**, 1458 (1987).
 [33] D. D. Reid, Ph.D. thesis, Wayne State University, 1995 (unpublished).
 [34] C. K. Kwan, W. E. Kauppila, R. A. Lukaszew, S. P. Parikh, T. S. Stein, Y. J. Wan, and M. S. Dababneh, *Phys. Rev. A* **44**, 1620 (1991).
 [35] S. P. Parikh, W. E. Kauppila, C. K. Kwan, R. A. Lukaszew, D. Przybyla, T. S. Stein, and S. Zhou, *Phys. Rev. A* **47**, 1535 (1993).
 [36] W. E. Kauppila, C. K. Kwan, T. S. Stein, and S. Zhou, *J. Phys. B* **27**, L551 (1994).
 [37] A. Surdutovich, J. Jiang, W. E. Kauppila, C. K. Kwan, T. S. Stein, and S. Zhou, *Phys. Rev. A* **53**, 2861 (1996).
 [38] T. T. Gien, *J. Phys. B* **23**, 2357 (1990).
 [39] William F. Egelhoff, Jr., *Phys. Rev. Lett.* **71**, 2883 (1993).